Adaptive network models of collective decision making in swarming systems

Li Chen, Cristián Huepe, and Thilo Gross

Phys. Rev. E **94**, 022415 — Published 18 August 2016

DOI: 10.1103/PhysRevE.94.022415

Adaptive network models of collective decision making in swarming systems

Li Chen*
Max Planck Institute for the Physics of Complex Systems, 01187 Dresden, Germay

Cristián Huepe
CHuepe Labs, 922 W 18th Place, Chicago, Illinois 60608, USA and
Northwestern Institute on Complex Systems, Northwestern University, Evanston, Illinois 60208, USA

Thilo Gross
Department of Engineering Mathematics, Merchant Venturers Building,
University of Bristol, Woodland Road, Clifton, Bristol BS8 ITR, United Kingdom

We consider a class of adaptive network models where links can only be created or deleted between nodes in different states. These models provide an approximate description of a set of systems where nodes represent agents moving in physical or abstract space, the state of each node represents the agent's heading direction, and links indicate mutual awareness. We show analytically that the adaptive network description captures a phase transition to collective motion in some swarming systems, such as the Vicsek model, and that the properties of this transition are determined by the number of states (discrete heading directions) that can be accessed by each agent.

PACS numbers: 05.90.+m, 89.75.Hc, 87.23.Cc

I. INTRODUCTION

Adaptive networks define a versatile class of models that have been recently applied to a wide variety of systems [1, 2]. They combine processes that change the structure of a network, such as growth or rewiring, with dynamics taking place on the network. This results in a feedback between topology and dynamics that can lead to different forms of self-organization. Following the pioneering work of Bornholdt and Rohlf [3] adaptive networks have been applied to a wide range of systems, including neural networks [4, 5], mobile sensor networks [6, 7], epidemics [8, 9], and the evolution of cooperation [10, 11], among many others.

In the study of adaptive networks, a special role is played by opinion formation models and, in particular, by the adaptive voter model and its variants [13–20]. The adaptive voter model describes the process through which a population of agents forms an opinion. A group of nodes representing agents are connected by links that describe social interactions. Each node is associated to a variable that can take values representing all possible opinions. At every iteration, the network is updated by propagating these values along the links (social adjustment) and by rewiring links (social segregation). One typically considers nodes that rewire their connections to surround themselves by like-minded agents that hold the same opinion. This common type of social dynamics is called *homophily*. Its opposite *heterophily*, where agents seek connections to different-minded agents [16], has received much less attention.

Extensions of the adaptive voter model have been recently proposed to describe collective motion in groups of animals [21, 22], a basic social phenomenon that occurs in a broad variety of species. Examples include insect swarms, fish schools, bird flocks, herds of quadrupeds [23–27], and even crowds of people [28]. Here, we will refer to all these, generically, as *swarming systems*. The process through which such systems self-organize into coordinated collective motion is still poorly understood. There has been much debate, for example, regarding the nature of the swarming transition that marks the onset of collective motion [26].

Most theoretical studies investigate swarming by either analyzing detailed agent-based models [29] or representing the swarm as a continuous medium [30, 31]. Adaptive network models provide an alternative route: the swarm is represented as an adaptive network by an approximation that captures the agents' headings and interactions but neglects their trajectories in space. In such models, each agent is represented by a node, its heading direction is treated as an internal state, and mutual awareness between two agents is represented by a link. But, there is no explicit representation of space, i.e. no variable keeps track of each agent's position in space.

Network swarming models are reminiscent of the adaptive voter model, where the subject of the opinion formation process is now the heading direction. However, a notable difference is that physical motion can lead both to the formation and dissolution of links to agents of different heading direction (Fig. 1). The adaptive swarming models thus constitute a third class of opinion formation systems comprising aspects of both homophily and heterophily. We refer to such systems as the *swarming systems class* of adaptive network models.

This application of voter-like models in the investigation of swarming was originally proposed [21] to model

*Electronic address: chenli@pks.mpg.de

experiments on locusts marching in a ring-shaped arena [32]. A slightly extended version of this model was later used to predict the outcome of decision-making experiments with fish [22].

We note that the swarming systems class of adaptive network models may also be relevant for other applications that consider motion in abstract (rather than physical) space. For instance, if translated into a social context, where different heading directions correspond to different opinions, it describes system individuals that both create or destroy social connections mainly with those who have a different opinion. While this is not the most common social dynamics, it may describe situations where original opinions are strongly valued and attract new social interactions but also create tensions within established interactions, leading to dissolution.

The previously proposed adaptive network models for swarming systems considered only cases where each agent was restricted to choose between two heading directions, corresponding to clock-wise or counter-clockwise motion in the circular arena [21] or to swimming towards one of two targets [22] in the collective decision-making experiment. These investigations thus focused on situations where the internal opinion state was a binary variable, akin to the adaptive voter model. While several multi-state extensions to the voter model have been explored [13, 19, 33, 34], the present paper is the first to analyze a similar extension for the swarming system class of adaptive network models. This extension is intuitive, as real swarms typically move in two or three-dimensional space, where the heading direction can be discretized into more than two node states.

In this paper we show that the swarming system class of adaptive network models displays a symmetry-breaking ordering transition that can be likened to collective motion. This transition can be either continuous or discontinuous, depending on the number of accessible states (e.g. the dimensionality of the embedding space).

The paper is organized as follows. Section II introduces the swarming system class of adaptive network models. Section III analyzes its mean field approximation. Section IV computes its analytical and numerical solutions. Section V compares our adaptive network results with the standard swarming transition to collective motion. Finally, Section VI presents our conclusions.

II. ADAPTIVE NETWORK SYSTEM

We consider a system of N nodes, representing agents, and links representing mutual awareness. Each node can be connected to any number of other nodes and has an internal variable that encodes the agents opinion state, or equivalently heading direction, from a set of M discrete states. For convenience, we denote the set of all possible opinion states by $\Omega = \{1, 2, ..., M\}$ and the complement of a given state X with respect to Ω by $\overline{\Omega}_{\{X\}} = \Omega \backslash \{X\}$. The initial states of the agents are drawn from Ω with equal probability.

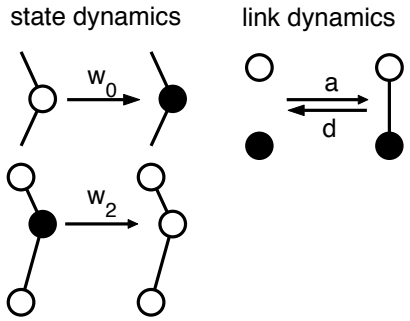

FIG. 1: Model illustration. The diagram presents nodes (circles) displaying two different opinions (black/white) out of M possible choices. The state dynamics (left column) consists of spontaneous flipping of individual nodes (top), and of three-body processes (bottom), with rates w_0 and w_2, respectively. The link dynamics (right column) consists of the creation and deletion of links only between nodes in different states, with rates a and d, respectively. These dynamics take place irrespective of any additional links, which may be present, but are not shown in this figure.

The network is initialized as an Erdős-Rényi random graph with initial mean degree $\langle k \rangle = 3$. We note, however, that this system has unique attractors and therefore the results obtained below are independent from these initial conditions.

The state of each node and the linking and unlinking dynamics are functions of continuous time. At each moment, there is a probability density (associated to the current configuration) for a transition to a different state and to link or unlink to other nodes. Specifically, the network then evolves in time as follows (see Fig. 1):

State dynamics — The state of each node is updated according to one of the following three processes. (i) Every node changes its state spontaneously at a rate w_0. In a spontaneous state change from state X the node picks one of the $M-1$ other states in $\overline{\Omega}_{\{X\}}$ with equal probability. Therefore, w_0 can be viewed as a coefficient that controls the "flipping noise", that is, the probability of spontaneously changing an agents opinion state (i.e. its heading direction). (ii) In every triplet of nodes $Y{-}X{-}Y$, where two nodes on the same state Y are linked to a single node on a different state X, the central node switches its state to Y with a probability that amounts to a net rate of w_2 transitions per triplet.

The state dynamics rules capture two intuitive processes: random noise and conforming to a local majority (an effect of the triplet process). It is also intuitive to include a pairwise process in which one individual convinces another individual of its opinion. However, some previous publications [15, 18, 19] have shown that this process does not have an impact on the deterministic dynamics at pair-level, i.e. in the thermodynamic limit it averages out and in smaller systems only acts as a small

additional source of noise. For the sake of simplicity we hence omit the pairwise interaction term in the present model.

Link dynamics — Links are established or removed between pairs of nodes that are in different states, with probabilities that amount to a net creation and deletion rates of a (per pair) and d (per link), respectively.

The numerical network simulations reported below were carried out using an event-driven (Gillespie) algorithm, which provides a statistically exact description of the continuous-time dynamics at the link level by using random numbers to determine not only if a state or link transition occurs, but also the time interval before it. Details of this implementation are provided in [35, 36].

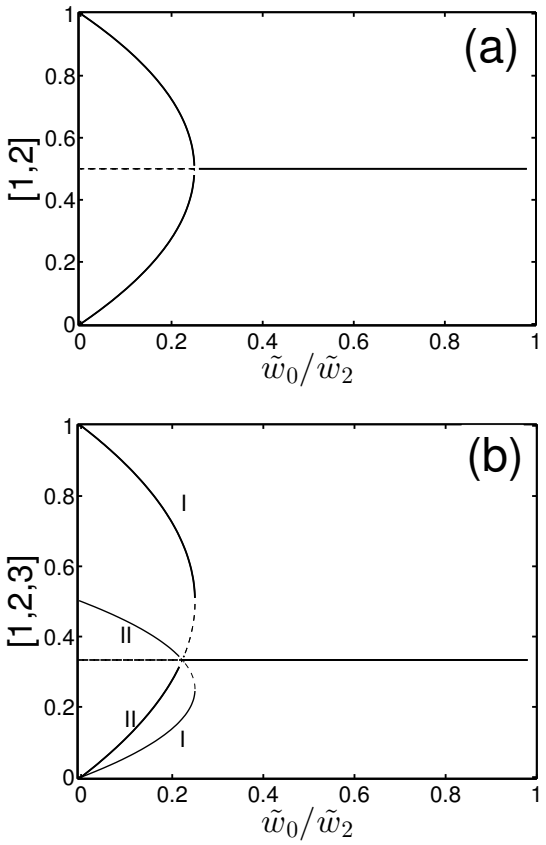

FIG. 2: Bifurcation diagram of the mean field approximation of the density of agents in each state as a function of normalized flipping noise $\tilde{w}_0/\tilde{w}_2$ in the $M = 2$ (a) and $M = 3$ (b) cases. The analysis reveals stable (solid) and unstable (dashed) branches of steady state solutions. The $M = 2$ case (a) undergoes a continuous transition in the form of a supercritical pitchfork bifurcation. The $M = 3$ case (b), presents two sets of stable solutions: one set (I) appears through a discontinuous transition and corresponds to a single majority opinion and two minority opinions with the same number of agents, the other set (II) results from a continuous transition and corresponds to two majority opinions with equal number nodes and a single minority opinion.

III. MEAN FIELD SOLUTION

Before carrying out an adaptive network analysis, it is instructive to gain some intuition by considering a mean field approximation. This approximation is equivalent to neglecting the link dynamics and assuming that the density of links connecting nodes in given states is proportional to the product of the densities of these states. While crude, it leads to a picture that is qualitatively similar to the adaptive network results described in Section IV, but using a much simpler mathematical description.

For simplicity, we denote by x the density of a given state and by y_i the density of each of the other $M-1$ states, as a function of continuous time, and whose evolution is governed by the dynamics in Section II with different rates. In principle one could now write the master equation of the system and then coarse grain this equation to derive the deterministic macro-level dynamics [37]. However, in the study of adaptive network models already a variety of related models has been explored and based on this experience it is possible to also write down the macroscopic equations in the deterministic limit directly. We find

$$\frac{\mathrm{d}x}{\mathrm{d}t} = \frac{w_0}{M-1}\left(\sum_{i=1}^{M-1} y_i\right) - w_0 x + w_2\langle k\rangle^2 \sum_{i=1}^{M-1}\left(x^2 y_i - y_i^2 x\right), \tag{1}$$

where $\langle k\rangle = \frac{1}{N}\sum_{j=1}^{N} k_j$ is the mean degree (i.e. the mean number of links per network node) and k_j is the number of links connected to node j.

In the equation the first two terms describe the gain and loss of nodes in state x due to the noise-induced spontaneous flipping, respectively, and the last term captures the gains and losses resulting from the triplet process. Two-body interactions do not appear in this equation because the corresponding terms cancel out due to the symmetry of the associated processes. The conservation of the total node density implies that $x + \sum_i y_i = 1$.

In numerical simulations of Eq. 1, we found that this system will either converge to a disordered (mixed) solution, where all densities are equal, or to an ordered state, where a single majority direction emerges and all other states have the same lower density. If we consider only solutions that follow this structure, we can thus make analytical progress by assuming $y_1 = y_2 = \ldots = y_{M-1} =: y$. This leads to the simplified system

$$\frac{\mathrm{d}x}{\mathrm{d}t} = \tilde{w}_0\,(y - x) + \tilde{w}_2\,(M-1)\left(x^2 y - y^2 x\right), \tag{2}$$

where we defined $\tilde{w}_0 = w_0$ and $\tilde{w}_2 = w_2\langle k\rangle^2$, for simplicity. We now compute the steady state solutions of the system by setting the left hand side of this equation to zero. Factorizing $y - x$, we obtain

$$0 = (y - x)[\tilde{w}_0 - \tilde{w}_2(M-1)xy]. \tag{3}$$

From this equation it is apparent that we get a symmetric

solution $x = y$ and asymmetric solutions that satisfy

$$xy = \frac{\tilde{w}_0}{\tilde{w}_2(M-1)}. \tag{4}$$

Using the normalization condition $(M-1)y + x = 1$, we find that the symmetric solution is given by $x = 1/M$, and the asymmetric pair is by

$$x = \frac{1}{2} \pm \sqrt{\frac{1}{4} - \frac{\tilde{w}_0}{\tilde{w}_2}}, \tag{5}$$

which is independent of the number of states M. The constant symmetric solution represents a disordered state where all heading directions are equally probable. The parabolic asymmetric solution with positive square root in Eq. (5) corresponds to the ordered state with single majority heading direction that we also found numerically, whereas the negative square root solution indicates a symmetry-broken solution with a single minority state, which we never observed in simulations.

As the flipping noise level is increased, the system undergoes a transition from the ordered to the disordered state (Fig. 2). Using elements of bifurcation theory [38], a direct visual inspection of this bifurcation diagram reveals the points at which the stability of these steady state branches must change. Bifurcations occur both at the rightmost points of the parabolas and at the intersection point of the different solutions.

The rightmost points of the parabola satisfy $\tilde{w}_0/\tilde{w}_2 = 1/4$, where the stable and unstable solution branches meet through in saddle-node bifurcation. The intersection of the two solutions occurs at $\tilde{w}_0/\tilde{w}_2 = (1-1/M)/M$ where a degenerate transcritical bifurcation takes place.

In the context of the original agent-based stochastic system, the bifurcation points correspond to phase transitions. For any $M > 2$, the destabilization of the mixed state occurs in a subcritical bifurcation, corresponding to a discontinuous transition. Only in the $M = 2$ case, the two types bifurcation points coincide at $\tilde{w}_0/\tilde{w}_2 = 1/4$, and a supercritical pitchfork bifurcation is formed, corresponding to a continuous transition.

A detailed stability analysis [39] of Eq. (2) verifies the results above and shows an additional set of stable solution branches (labeled by II in Fig. 2). In these branches two majority opinions are represented in an equal number of nodes and while a single minority opinion is held by a smaller number of nodes. However, in the next section we show that the stability of branches is lost when a more accurate approximation is used. This suggests that the stability of the 2-majority-1-minority branches is a spurious result of the mean field approximation, which appears due to an excessive reduction of the dimensionality of the state space. In the full system these branches are thus unstable to certain perturbations that involve a dynamical redistribution of links, which is not captured by the mean field.

IV. ADAPTIVE NETWORK SOLUTION WITH PAIR-LEVEL CLOSURE

We now derive a system of equations that takes the dynamics of link densities into account, using a moment expansion [40]. The basic idea of this expansion is to write differential equations that capture the density of small subgraphs. These densities are also called network moments. Each subgraph can be classified by its order, which is equal to the number of links it contains. For example, if we have three distinct states $X,Y,Z \in \Omega$, the density of nodes in the X state, denoted by $[X]$, is a zeroth-order moment; the per-capita density of $X-Y$ linked pairs $[XY]$, a first-order moment; and the X–Y–Z triplet density $[XYZ]$, a second-order moment.

Note that these motifs are also counted even when they are found within a larger network structure, that is, regardless of any other links that the nodes involved may have or of any other motifs (of any order) that they may be part of. This implies that, for example, in an isolated chain-like network structure $X-Y-X$ we would count two X nodes, one Y node, two $X-Y$ pairs, and an $X-Y-X$ triplet, and that each of these motifs will follow the corresponding transition rates detailed above. With these definitions, the dynamics of the zeroth and first order moments are captured by

$$\frac{\mathrm{d}}{\mathrm{dt}}[X] = \frac{w_0}{M-1}\Big\{\sum_{Y\in\overline{\Omega}_{\{X\}}}[Y] - (M-1)[X]\Big\} + w_2 \sum_{Y\in\overline{\Omega}_{\{X\}}}\Big\{[XYX]-[YXY]\Big\}, \tag{6}$$

$$\frac{\mathrm{d}}{\mathrm{dt}}[XX] = \frac{w_0}{M-1}\Big\{\sum_{Y\in\overline{\Omega}_{\{X\}}}[XY] - 2(M-1)[XX]\Big\} + w_2 \sum_{Y\in\overline{\Omega}_{\{X\}}}\Big\{2[XYX]+3[{}^{X}Y_{X}^{X}]-[{}^{X}X_{Y}^{Y}]\Big\}, \tag{7}$$

$$\begin{aligned}\frac{\mathrm{d}}{\mathrm{dt}}[XX'] = {} & \frac{w_0}{M-1}\Big\{2([XX]+[X'X']) + \sum_{Y\in\overline{\Omega}_{\{X,X'\}}}([XY]+[X'Y]) - 2(M-1)[XX']\Big\} + w_2\Big\{-2[XX'X] - 2[X'XX'] + [{}^{X}X_{X'}^{X'}] \\ & + [{}^{X'}X'^{X}_{X}] - 3[{}^{X'}X_{X'}^{X'}] - 3[{}^{X}X'^{X}_{X}] + \sum_{Y\in\overline{\Omega}_{\{X,X'\}}}\big([{}^{X'}Y_{X}^{X}]+[{}^{X}Y_{X'}^{X'}]-[{}^{X}X'^{Y}_{Y}]-[{}^{X'}X_{Y}^{Y}]\big)\Big\} + a[X][X'] - d[XX'],\end{aligned} \tag{8}$$

where $X, X' \in \Omega$ (with $X \neq X'$), and $[{}^{X}Y_{Z}^{W}]$ denotes the density of motifs with a central node in state Y connected

to three other nodes in states X, W, and Z.

In the equations above, the first right-hand side term corresponds to noise-driven state dynamics and the second, to three-body interactions. The remaining terms in Eq. (8) result from the link creation and deletion processes. These expressions summarize a larger system of equations, with (6), (7) and (8) representing M, M, and $M(M-1)/2$ equivalent equations, respectively.

If we had included the common two-body opinion transmission process in our model, the corresponding terms would vanish in the zeroth-order moment dynamics due to the symmetry of the associated processes. Higher-order terms do include two-body interaction terms, but their effect amounts to an additional noise source that changes the number of linked pairs in different states. We verified numerically that this effect is small in our model when compared to the effect of the explicit linking and unlinking dynamics, and that it does not produce any qualitative changes in the resulting stationary solutions or their stability.

Note that each equation describing the dynamics at a given order involves higher order terms. We thus need to close the system through a moment closure approximation. We use a pair-level closure [8, 41] of the form

$$[XYZ] = \frac{h([XY])h([YZ])}{h([XYZ])}\frac{[XY][YZ]}{[Y]},$$

$$[{}^{X}Y^{Z}_{W}] = \frac{h([XY])h([YZ])h([YW])}{h([{}^{X}Y^{Z}_{W}])}\frac{[XY][YZ][YW]}{[Y]^2},$$

where $h([XY]) = 1+\delta_{XY}$, $h([XYZ]) = 1+\delta_{XZ}$ and $h([{}^{X}Y^{Z}_{W}]) = 1+\delta_{XZ}+\delta_{XW}+\delta_{ZW}+\delta_{XZ}\delta_{ZW}+\delta_{XW}\delta_{ZW}$, with δ the Kronecker delta.

These pair-level closure expressions can be derived by writing the statistical estimates of triplet and quadruplet densities that would result from a random combination of the existing densities of states and pairs (i.e. of zeroth- and first-order motifs, respectively). Thus these approximations neglect longer-than-pair correlations in the system. This approximation is known to be problematic close to fragmentation transitions [18, 19], however this is not an issue in the present model (see also [20] for a detailed discussion of the failure of this type of approximation).

To make analytical progress, we assume that the creation and deletion rates of every type of link cancel each other independently in the stationary solution, i.e. $a[X][X']=d[XX']$. This is the simplest way for the system to present a stationary solution, since otherwise the excess of link creation or deletion would have to be exactly compensated by changes in node states that, at the same time, keep the density of all moments constant. We confirm numerically the validity of this assumption in Figs. 3a and 3b, where we show that our final results match well the direct agent-based simulations of the full network dynamics.

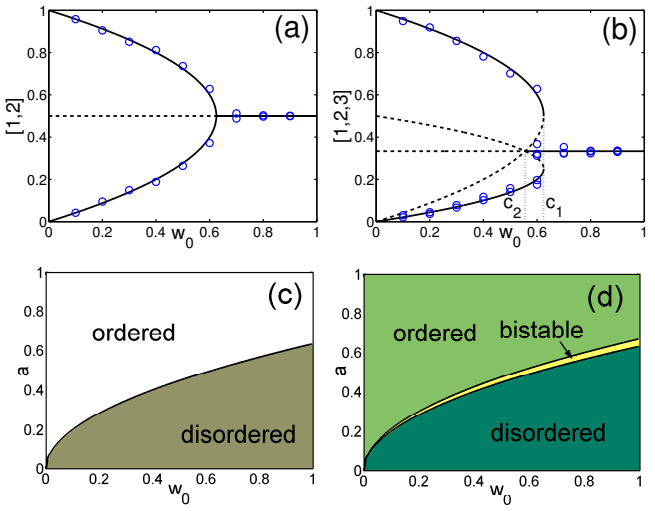

FIG. 3: (Color online). Bifurcation diagrams (a, b) and phase diagrams (c, d) of adaptive network systems with $M = 2$ (left) and $M = 3$ (right) available states per node. The bifurcation diagrams (top) show the density of nodes in a given state for the stable (solid) and unstable (dashed) stationary solutions. In both diagrams, the system undergoes a transition from a disordered solution to an ordered one as the noise level w_0 is decreased. For $M = 2$ (a) this transition occurs through a supercritical pitchfork bifurcation and for $M = 3$ (b), through a transcritical one, corresponding to a continuous or a discontinuous transition, respectively. Analytical results using a pair-level closure approximation (lines) are in good agreement with numerical network simulations (circles) using $N = 10^4$ nodes. The phase diagrams (bottom) display the ordered, disordered, and bistable regions as a function of noise w_0, and of link creation rate a, for $M = 2$ (c) and $M = 3$ (d). We note that the bistable region is only present in the $M \geq 3$ case. Parameters: $a = 0.5$ (only in top panels), $w_2 = 0.2$, $d = 0.1$.

In analogy to the mean field case, we assume that all states have identical densities except for a single focal state. We denote by $[x]$ the density of nodes in this focal state and by $[j]$ the density of each of the other $M-1$ states. We can then replace the pair-level approximations into Eq.(6) and use these assumptions and notation to obtain

$$\frac{d[x]}{dt} = w_0\left([j]-[x]\right) + \frac{w_2}{2}\left(M-1\right)[xj]^2\left(\frac{1}{[j]}-\frac{1}{[x]}\right). \quad (9)$$

By using the assumption $a[X][X'] = d[XX']$, introduced above, and imposing the conservation law $\sum_{i=1}^{M}[i] = 1$, we find the stationary solutions

$$[x] = [j] = 1/M \quad (10)$$

and

$$[x] = \frac{1 \pm \sqrt{1 - w_0/c_1}}{2}, \quad (11)$$

$$[j] = \frac{1 \mp \sqrt{1 - w_0/c_1}}{2(M-1)}. \quad (12)$$

Here, $c_1 = w_2 a^2/(8d^2)$ and Eq. (12) represents $M-1$ identical equations for the node densities of all states other than x.

The results of the analysis (Fig. 3) are similar to those obtained with the mean field approximation: at low noise the disordered state becomes unstable and stable branches appear that correspond to the symmetry-broken solution. However, there two differences. First, only the ordered solution that has one majority opinion and $M-1$ minority opinions is stable; the reversed case (Set II in Fig. 2) with one minority opinion and $M-1$ majority opinions is unstable. Second, the bifurcation points now depend on the density of linked pairs, and are therefore functions of the link creation and deletion rates. The saddle-node bifurcation (for $M > 2$) where the ordered states vanish now occurs at c_1, whereas the transcritical bifurcation where the disordered state loses its stability is at

$$c_2 = \left[1 - \left(\frac{M-2}{M}\right)^2\right] c_1. \qquad (13)$$

We therefore have $c_2 < c_1$ for all systems with more than two available states. Thus, the transition is generally of first order and has a bistable region in the w_0 interval given by $c_2 < w_0 < c_1$. In the limit of a large number of possible states, $c_2 \to 0$ and the region of bistability extends to the origin. A continuous transition is only observed in the special case of two opinions, where $M = 2$ implies $c_1 = c_2$ and the two transitions coincide, to form a pitchfork bifurcation.

The analytical predictions are in good agreement with results from large agent-based simulation runs (cf. Fig. 3 panels a,b). Only near the critical points a small difference is observed, which may be due to the moment closure approximation in our analytical calculations or to finite size effects in our agent-based simulations.

V. COMPARISON TO THE SWARMING TRANSITION

In this Section, we relate the ordering transition described above to the collective motion transition observed in swarms by interpreting our adaptive network model as a simplified version of a Vicsek model [26]. This is the most commonly used minimal model in the study of swarming systems. It describe self-propelled particles moving at a constant speed that tend to align their heading directions when interacting. We will consider a simplified version of the Vicsek algorithm (which we refer to as *the discrete Vicsek model*) where agents can only move in discrete heading directions and the agent positions are not tracked. For this purpose, each node is interpreted as a self-propelled agent, its state as its heading direction, and linked nodes as interacting agents. An advantage of this approach is that it does not require specifying the details of the interactions. While collective motion

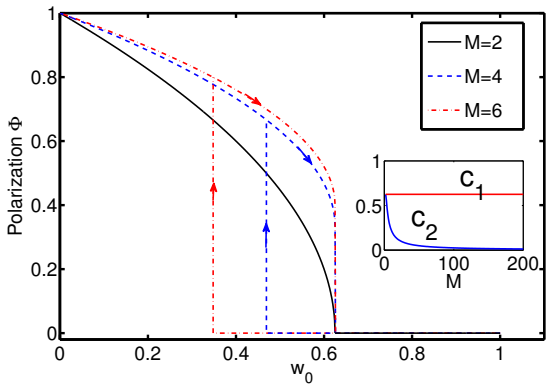

FIG. 4: (Color online). Bifurcation diagrams of the alignment order parameter Φ defined in Eq. (15) as a function of noise w_0 for the adaptive network model with pair-level closure described in Section IV, when interpreted as the discrete Vicsek model introduced in Section V (see text). The curves were computed using Eqs. (10-12) for $M = 2$, 4, and 6 potential heading directions, corresponding to $D = 1$, 2, and 3 dimensions, respectively. For $M = 2$, the transition is continuous. For $M > 2$, the critical value of the control parameter where the $\Phi = 0$ branch loses stability (c_2) becomes smaller than point where the upper branch vanishes (c_1). This results in a discontinuous transition and a region of bistability, which gives rise to the hysteresis cycles indicated by the arrows. The inset displays c_1 and c_2 as a function of M; the bistable region is broader for larger M values.

can result from a broad variety of interactions (such as aligning [29], attraction-repulsion [42, 43], and escape-pursuit [44]), the adaptive-network perspective can treat all of these equally by focusing on the exchanges of information that lead to consensus on the collective heading direction, without considering the details of the interactions. In particular, if we assume that interactions can only occur within a given distance, the limit case studied in this paper (where the linking and unlinking rates between agents in the same state is set to zero) can be mapped to a situation where agents that advance in a common direction do not change their relative positions and therefore do not create or destroy interactions between them. We also focus on the simplest limit case where the linking and unlinking rates (corresponding here to encounter and disbanding rates at which agents start and stop interacting with each other) are constant and equal for all agents in different states (i.e. with different headings). Note that the adaptive network model that we consider in this paper defines an equal probability of spontaneously switching to any new heading state, given by the single rate w_0 introduced in Section II. In the context of swarms, this implies an equal probability of turning perpendicular to or opposite to the current heading direction. Although this is not likely the case in real swarms, there is no known general rule on how to define these probabilities, which must depend on the specificities of the system considered. In order to man-

age simpler expressions and as a first effort in our model analysis, we therefore consider here the case with a single w_0 value for the probability of switching to any heading direction, leaving the analysis of using different rates for different turning angles for future work.

In order to compare our adaptive network system to collective motion, we start by associating each node state $[h]$ with an agent's heading $\hat{v}$ in a space where they can only move in discretized directions that are parallel or perpendicular to each other. Each $\hat{v}$ is thus a unit vector pointing in a direction that is either the same, opposite, or orthogonal to all others. The number of potential headings M therefore depends on the dimensionality of the space, with $M = 2$ in one dimension, $M = 4$ in two dimensions, $M = 6$ in three dimensions and, in general, $M = 2D$ in D dimensions.

The usual polarization order parameter used to describe the degree of alignment and of collective motion in the standard Vicsek model and other swarming systems [26] is given by

$$\Phi = \frac{1}{N}\left|\sum_{i=1}^{N}\hat{v}_i\right|, \tag{14}$$

where N is the total number of agents and $\hat{v}_i$ is a unit vector indicating the heading direction of agent i [26]. With this definition, $\Phi = 1$ if all agents are perfectly aligned and swarming in the same direction, whereas $\Phi = 0$ if they are randomly oriented.

In the discretized space with only orthogonal heading directions that we consider here, Φ can be expressed as

$$\Phi = \sqrt{\sum_{h=1}^{M/2}\left([2h]-[2h-1]\right)^2}. \tag{15}$$

Here the sum is over the $D = M/2$ dimensions of the space that contains the corresponding swarm. The term $[2h]-[2h-1]$ is the mean speed of the swarm along one of the axes (if each agent is defined to have unit speed), where $[2h]$ is the total fraction of agents heading in the positive axis direction and $[2h-1]$ is the total fraction of agents heading in the opposite (negative axis) direction. This relationship allows us to plot the polarization order parameter Φ as a function of w_0, which serves as a proxy for the amount of noise in the agent motion (Fig. 4).

In the context of swarms, the bifurcations computed above correspond to ordering phase transition to collective motion. For agents moving in one-dimensional space ($M = 2$), the transition of the discrete Vicsek model is continuous (second order), whereas for agents moving in more dimensions ($M \geq 4$), the transition is discontinuous (first order). A region of bistability occurs for $M \geq 3$ and is broader for higher values of M (Fig. 4 inset).

Although the adaptive network approach includes several approximations, the results above provide insights into the more complex problem of understanding general features of the transition to collective motion in swarms.

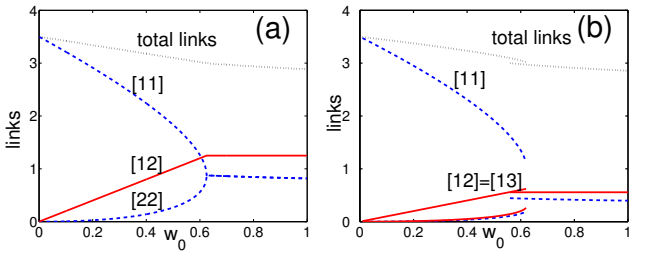

FIG. 5: (color online). Per-capita density of linked pairs as a function of noise w_0 for the adaptive network model with pair-level closure described in Section IV (see text). All curves were obtained analytically from Eqs. (10-12), and the assumption $a[X][X'] = d[XX']$, for $M = 2$ (a) and 3 (b) using the same parameters as in the corresponding bifurcation diagrams in Fig. 3. Blue dashed lines: Density of linked pairs with both nodes in the same state of majority (labeled [**11**]) or minority opinion ([**22**] and [**33**], the lowest branch at left side in both plots). Red solid lines: Density of linked pairs with one node in the majority and one in the minority opinion ([**12**] and [**13**]), or both in the minority opinions ([**23**], the lower red one at left side in (b)). Black dotted lines: Total density of linked pairs. The bifurcation features displayed in Fig. 3 are mirrored here in these link density plots.

The question of whether the actual swarming transition to collective motion is continuous or discontinuous, for example, has been the subject of intense debate [29]. While in the initial numerical explorations the transition appeared to be continuous (second order), it was later shown through theoretical arguments and large-scale numerical simulations that it is, in fact, discontinuous (first order) and has a bistable transition region where ordered and disordered swarming states coexist [29, 45, 46].

The results presented in Fig. 4 would suggest that, generically, this transition should be continuous in one dimension and discontinuous in two or three dimensions, with a more prominent bistable region in the 3d case.

To our knowledge, there has been no systematic analysis of the properties of the ordering transition as a function of the embedding space dimensionality for different types of swarming models. In one dimension, different approaches have concluded that the transition is either absent or first order [47–50]. In two dimensions, the transition has been much better studied and shown to be first order, as in three dimensions, but the size of their bistable regions has not been compared [26, 31].

We can further examine the connection between the adaptive network model and swarming systems by considering the per-capita densities of linked pairs displayed in Fig. 5. These match the interaction frequencies that are expected to occur in swarms. For example, the total number of links decreases monotonically with noise level, which corresponds to the observation that higher noise values will produce less clustering and therefore fewer interactions between agents in swarming systems [26, 51]. We also see that the density of heterophilic links [**12**] (and [**13**] in the $M = 3$ case) increases with noise. This

can be explained by an increasing rate of encounters at higher noise levels.

Furthermore, we find that for all cases with $M > 2$ (such as the $M = 3$ case displayed in the figure) the ordered branch's density of heterophilic links [**12**] and [**13**] continues to increase as a function of noise in the bistable region, where it becomes higher than that of the disordered branch. Despite this high number of heterophilic links, the ordered branch persists because the density of homophilic links [**11**] is also high. This can be related to bistable regions in swarms, where it is known that a higher density of interactions between agents in the majority heading state, which corresponds to the formation of high-density bands (oriented perpendicular to the heading direction) in two or more dimensions stabilizes the ordered state [45, 46], leading to a bistable region and thus to a discontinuous transition. This analogy could provide an alternative way to understand the details of the bifurcation as a function of the dimension of the embedding space.

VI. CONCLUSIONS

In this paper, we analyzed the swarming systems class of adaptive network models, where links can only be created or deleted between nodes in different states. We showed analytically that, in the mean field and adaptive network (with pair-level closure) approximations examined here, this class displays a symmetry-breaking transition with properties that depend on the number of states M accessible to each node. If $M = 2$, the transition occurs through a supercritical pitchfork bifurcation; if $M \geq 3$, through a subcritical one. Consequently, only this latter case displays a bistable region near the bifurcation point. Note, however, that previous work [21] had shown that bistable solutions can also be obtained in the $M = 2$ case if we allow link creation and deletion processes to occur between nodes in the same state, a situation that was not studied here.

The results above, taken together, provide insights on a potential direct connection between link dynamics, their dependence on internal states, and the resulting properties of this type of symmetry-breaking transitions.

The parallels between the adaptive-network approach presented here and agent-based dynamics are not restricted to swarming systems. They can be extended to any group of agents moving in an abstract phase space with similar dynamical rules. These rules must consider agents with an internal state (as the heading direction in the swarming case) that determines their trajectory in this phase space, in which their relative positions determine whether they interact. It is thus conceivable that the model proposed may be extended to study social processes involving heterophily, such as the diffusion of innovations and technologies [52] or job seeking through weak interpersonal ties [53].

Acknowledgements

We would like to thank Gerd Zschaler and Güven Demirel for their assistance in using the XPPAUT and largetnet library. The work of CH was supported by the US National Science Foundation under Grant No. PHY-0848755.

Data Statement

This work does not use research data.

[1] T. Gross and B. Blasius, J. R. Soc. Interface **5**, 259 (2008).
[2] *Aaptive Networks: Theory, Models and Applications*, edited by T. Gross and H. Sayama, (Springer, New York, 2008).
[3] S. Bornholdt and T. Rohlf, Phys. Rev. Lett. **84**, 6114 (2000).
[4] A. Levina, J. Herrmann, and T. Geisel, Nat. Phys. **3**, 857 (2007).
[5] C. Meisel and T. Gross, Phys. Rev. E **80**, 061917 (2009).
[6] T. E. Gorochowski, M. Di Bernardo, and C. S. Grieson, Complexity, **17**, 18 (2012).
[7] P. Ogren, E. Fiorelli, and N. E. Leonard, IEEE Trans. Automatic Control, **49**, 1292 (2004).
[8] T. Gross, C. Dommar D' Lima and B. Blasius, Phys. Rev. Lett. **96**, 208701 (2006).
[9] L. B. Shaw and I. B. Schwartz, Phys. Rev. E **77**, 066101 (2008).
[10] J. M. Pacheco, A. Traulsen, and M. A. Nowak, Phys. Rev. Lett. **97**, 258103 (2006).
[11] A.-L. Do, L. Rudol,f and T. Gross, New J. Phys. **12**, 063023 (2010).
[12] For more information please visit the adaptive networks wiki http://adaptive-networks.wikidot.com.
[13] P. Holme and M. E. J. Newman, Phys. Rev. E **74**, 056108 (2006).
[14] S. Gil and D. H. Zanette, Phys. Lett. A **356**, 89 (2006).
[15] M. G. Zimmermann, V. M. Eguiluz, and M San Miguel, Phys. Rev. E, **69**, 065102 (2004).
[16] D. Kimura and Y. Hayakawa, Phys. Rev. E **78**, 016103 (2008).
[17] F. Vazquez, V. M. Eguíluz, and M. S. Miguel, Phys. Rev. Lett. **100**, 108702 (2008).
[18] G. A. Böhme and T. Gross, Phys. Rev. E **83**, 035101(R) (2011).
[19] G. A. Böhme and T. Gross, Phys. Rev. E **85**, 066117 (2012).
[20] G. Demirel, R. Prizak, P. Reddy, and T. Gross, Eur. Phys. J. B **84**, 541 (2011).
[21] C. Huepe, G. Zschaler, A.-L. Do, and T. Gross, New J. Phys. **13**, 073022 (2011).
[22] I. D. Couzin, C. C. Ioannou, G. Demirel, T. Gross, C. J.

Torney, A. Hartnett, L. Conradt, S. A. Levin, and N. E. Leonard, Science **334**, 1578 (2011).
[23] I. D. Couzin and J. Krause, Adv. Stud. Behav. **32**, 1 (2003).
[24] J. Toner, Y. Tu, S. Ramaswamy, Annals of Phys. **318**, 170 (2005).
[25] D. J. T. Sumpter, *Collective Animal Behavior* (Princeton University Press, New Jersey, 2010).
[26] T. Vicsek and A. Zafeiris, Phys. Rep. **517**, 71 (2012).
[27] W. Bialek, A. Cavagna, I. Giardina et al., Proc. Natl. Acad. Sci. USA. **109** (2012).
[28] D. Helbing, Rev. Mod. Phys. **73**, 1067 (2001).
[29] T. Vicsek, A. Czirók, E. Ben-Jacob, I. Cohen, and O. Shochet, Phys. Rev. Lett. **75**, 1226 (1995).
[30] J. Toner and Y. Tu, Phys. Rev. Lett. **75**, 4326 (1995).
[31] J. Toner and Y. Tu, Phys. Rev. E **58**, 5828 (1998).
[32] J. Buhl, D. J. T. Sumpter, I. D. Couzin, J. J. Hale, E. Despland, E. R. Miller, and S. J. Simpson, Science **312**, 1402 (2006).
[33] G. Deffuant, F. Amblard, G. Weisbuch, and T. Faure, J. Artificial Societies and Social Simulations, **5**, 4 (2002).
[34] F. Shi, P.J. Mucha, and R. Durrett, Phys. Rev. E **88**, 062818 (2013).
[35] D. T. Gillespie, J. Phys. Chem., **81**, 2340 (1977).
[36] G. Zschaler and T. Gross, Bioinformatics, **29**, 277 (2013).
[37] C. T. Bauch, J. Math. Biol. **45**, 375 (2002).
[38] Y. A. Kuznetsov, *Elements of Applied Bifurcation Theory* (Second ed.), (Springer, 1998).
[39] The direct bifurcation analysis is conducted by using the software XPPAUT, which computes the detailed bifurcation diagram of a given set of ordinary differential equations. XPPAUT was developed by G. Bard Ermentrout, and is available at www.math.pitt.edu/∼bard/xpp/xpp.html for free.
[40] G. Demirel, F. Vazquez, G. A. Böhme, and T. Gross, Physica D **267**, 68 (2013).
[41] M. J. Keeling, D. A. Rand, and A. J. Morris, Proc. R. Soc. Lond. B **264**, 1149 (1997). M. J. Keeling and K. T. D. Eames, J. R. Soc. Interface **2**, 295 (2005).
[42] E. Ferrante, A. E. Turgut, M. Dorigo, and C. Huepe, New J. Phys., **15**, 095011 (2013).
[43] E. Ferrante, A. E. Turgut, M. Dorigo, and C. Huepe, Phys. Rev. Lett., **111**, 268302 (2013).
[44] P. Romanczuk, I. D. Couzin, and L. Schimansky-Geier, Phys. Rev. Lett., **102**, 010602 (2009).
[45] G. Grégoire and H. Chaté, Phys. Rev. Lett. **92**, 025702 (2004).
[46] H. Chaté, F. Ginelli, G. Grégoire, and F. Raynaud, Phys. Rev. E **77**, 046113 (2008).
[47] A. Czirók, A-L Barabási, and T. Vicsek, Phys. Rev. Lett. **82**, 209 (1999).
[48] O. J. O'Loan and M. R. Evans, J. Phys. A: Math. Gen. **32** L99 (1999).
[49] A. Kolpas, J. Moehlis, and I. G. Kevrekidis, P. Natl. Acad. Sci. USA **104**(14), 5931 (2007).
[50] A. P. Solon and J. Tailleur, Phys. Rev. Lett. **111**, 078101 (2013).
[51] C. Huepe and M. Aldana, Phys. Rev. Lett. **92**(16), 168701 (2004).
[52] E. M. Rogers, *Diffusion of innovations (5th edition)*, (Free press, New York, 2003).
[53] M. Granovetter, Am. J. Sociol. **78**, 1360 (1973).